

The 9 October 1963 Vajont Catastrophe from the Point of View of the WWSSN-LP Recordings of the TRI-117 Station, Trieste, Italy

Stefano Parolai¹, Denis Sandron^{*1}, and Alessandro Rebez¹



Abstract

In this study, we analyze the seismic signal generated by the 1963 Vajont catastrophic landslide recorded at the Worldwide Standardized Seismographic Station Network-Long Period station of Trieste (Italy). The landslide (nearly 260–270 million m³) invaded an artificial reservoir designed for electrical production, and generated a 220 m high wave that flowed over the dam and claimed the lives of approximately 2000 people. The original seismograms have been digitized and analyzed using time–frequency tools and numerical simulations. The results indicate that a seismic signal comparable to that generated by an *M*_s 3.7 earthquake was generated by the landslide. Furthermore, the calculated nearly 2×10^{14} J of frictional energy, considering the known parameter of the mass movement, is compatible with a friction coefficient of 0.29, in excellent agreement with the values from previous studies. The seismic efficiency that we calculate (1.12×10^{-4} – 4.45×10^{-4}), also taking into account available data on the landslide, is within the range of values previously noted in literature. Finally, via the numerical simulations and adopting an ad hoc crustal model for the area, the origin time of the event is estimated at 21 hr 41 min 42 s UTC. The results confirm the importance of the re-analysis of analog seismograms with modern tools within a multihazard context.

Introduction

On the evening of the 9 October 1963, a catastrophic landslide occurred on the northern slope of Mount Toc (northeastern Italy). A rockmass of around 260–270 million m³ collapsed into the artificial reservoir designed for electric power production, reaching a maximum velocity of 20–30 m/s, generating a 220 m high wave (Alonso *et al.*, 2010) that flowed over the 276 m height dam (which stood without bursting) and swept into the “Piave” valley below, claiming the lives of approximately 2000 people (Petronio *et al.*, 2013). At that time, over US\$16 million (roughly equivalent to 370 million U.S. dollars nowadays) was paid in civil lawsuits brought forward for personal injury and death. Although there is extensive literature focusing on this multihazard catastrophe (e.g., Dykes and Bromhead, 2018, and references therein) that shed some light on, some controversy remains with regard to the cause and impact of this disaster. Some previous studies have considered the seismic signal signature recorded by different seismometers around Europe. In particular, Caloi (1966) used the seismic recordings up to 2500 km distance to identify the waves generated by the landslide, to estimate its origin time (fixed at 21 hr 41 min 30 s UTC) and, using the station located in Rome, to provide an

estimate of the energy released as seismic waves, which he calculated to be 2×10^{11} J. Furthermore, Caloi (1966) first recognized the presence of two groups of perturbations on the seismogram, separated by nearly 30 s, that was explained as being due to the rock sliding and the drop of the mass of water (estimated to be nearly 25–30 million m³) spilling over the dam. In particular, the second event, simply looking at the recording of its timing, apparently had higher energy. Among the seismological stations existing at the time of the disaster, there was the station of Trieste, TRI-117 (Fig. 1a), managed by the National Institute of Oceanography and Applied Geophysics (OGS) (Fig. 1b) and installed in Borgo Grotta Gigante (about 12 km from Trieste) just a few months before (29 July 1963) the Vajont event and belonging to the Worldwide Standardized Seismographic Station Network (WWSSN; Sandron *et al.*, 2015). Because the seismological bulletins edited by OGS in

1. National Institute of Oceanography and Applied Geophysics—OGS, Sgonico, Italy,
 

*Corresponding author: dsandron@inogs.it

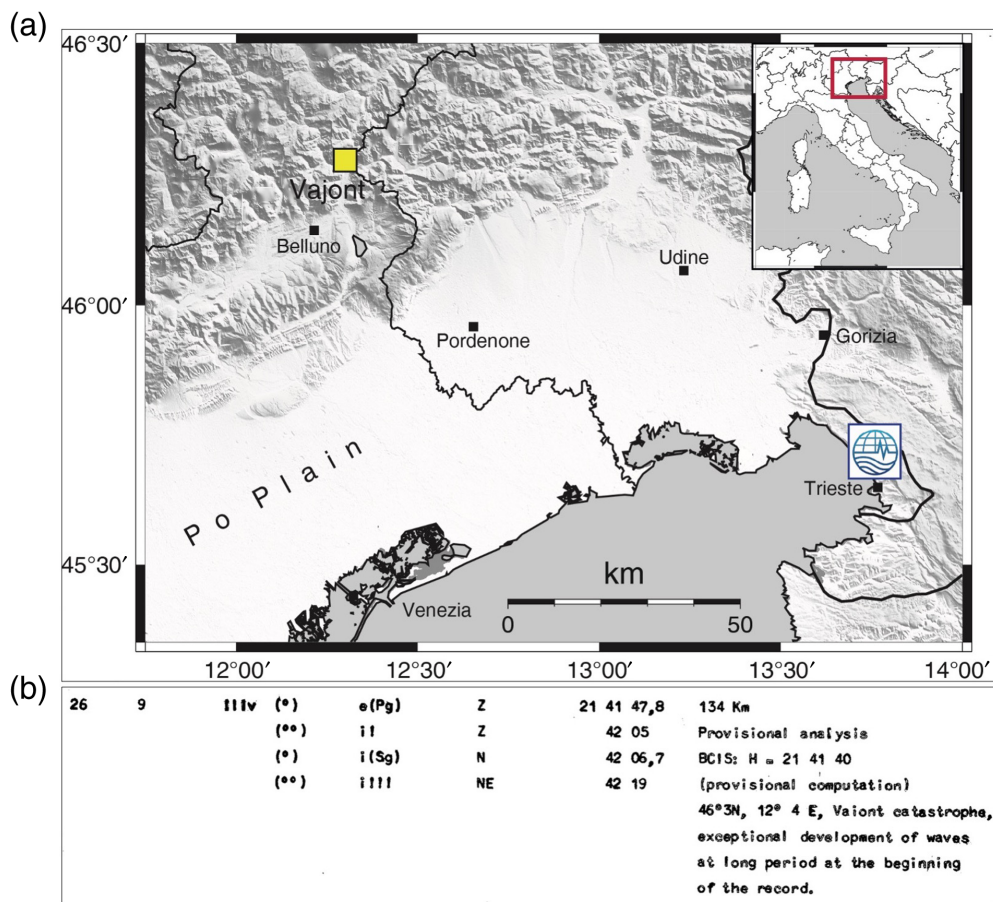


Figure 1. (a) Vajont dam is located 134 km northwest of the TRI-117 Worldwide Standardized Seismographic Station Network (WWSSN) installed at the National Institute of Oceanography and Applied Geophysics (OGS) near Trieste (northeast Italy). In the top right inset map the position of the study area (red box) in the Italian context. (b) Screenshot taken from the TRI-117 WWSSN station bulletin of 9 October 1963 edited by OGS. The color version of this figure is available only in the electronic edition.

1963 contained information on the Vajont catastrophe (Fig. 1b), and the original seismograms recorded by the TRI-117 station on paper are still available (Fig. 2a), we first searched for the possible recordings of the Vajont disaster, and, once they were found, they were digitized (Sandron *et al.*, 2014). The availability of the digitized seismograms offered new opportunities for analysis and is reported in this study. First, after having corrected the recordings considering the seismometer response, to obtain the original (although still band-pass filtered) ground displacement, we re-estimate the magnitude of the event and the efficiency of seismic-wave excitation of both the landslide and the drop of the water mass. Second, we applied a time–frequency analysis to the digital seismograms to better understand the sequence of the event and the overlapping of seismic phases at the station. Finally, we show the results of an attempt to model the observed seismogram using a source model compatible with the observations. The numerical simulations also allowed us to re-estimate the origin time of the event.

The TRI-117 Seismograms

The Trieste TRI-117 station was equipped with a three-component long-period (Ewing-Press) and short-period (Benioff) seismographs. The long-period electrodynamic seismometer was tuned to a free period of 15 s, with magnification 3000, and a long-period mirror galvanometer with a free period of 100 s (Peterson and Hutt, 2014). The WWSSN seismograms were recorded on photographic paper rotating on a drum (Fig. 2b). Figure 3 shows the original recordings of the Vajont event made by the station’s long-period seismometer. The short-period recordings appeared to be noisy and have not been used in the following analysis, except for a re-reading of the duration time of the landslide-related event for a comparative estimation of the magnitude. The WWSSN TRI-117 remained operational until 1996. Clear perturbations occurring after 21 hr 40 min UTC are shown on the recordings of all components. The largest peak-to-peak amplitude

is of 0.227 m on the north–south component, which roughly represents the transverse component of motion, and is obtained after the digitization procedure described in the following and interpolating in the small time interval (a few seconds) in which the waveform was clipped. Two main events are recognizable (separated by nearly 30 s) on the vertical (Z) component, with the second one, in agreement with Caloi (1966), showing a higher amplitude.

The analog seismograms have been scanned from the original daily sheets into 600 dpi gray scale images and then digitized using the software Teseo2 (Pintore *et al.*, 2005). For each seismogram, we chose a time-window length of 12 min, starting from 2 min before the origin time (time mark 21 hr 40 min UTC). In the first step, the digitization was done manually, trying to insert as many points as possible to follow the course of the track. Then, starting from the scattered points, it was possible to automatically resample the signal with a fixed sampling step of 3 samples per second, limiting the exploitable

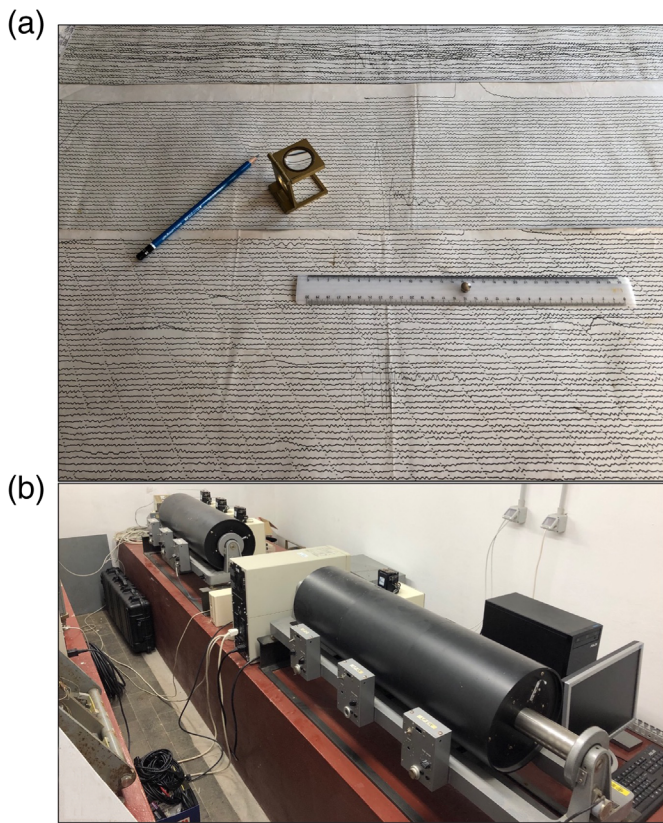


Figure 2. (a) Original daily paper sheets (three components) with the seismograms recorded by the TRI-117 WWSSN station on 9 October 1963; (b) the two original drums (long and short periods) installed at OGS. Note that the instruments (at the time not operational) are still located in the original positions as installed in 1963. Over the years, the recording equipment was changed switching from recording on photographic paper to recording on thermal paper. Between 2003 and 2009, the entire building in which the instruments are installed was renovated, but the instrument room was not modified to ensure its original condition. The color version of this figure is available only in the electronic edition.

frequency band to an upper limit of 1.5 Hz. In a small time interval (a few seconds) in which the North-South waveform was clipped, an interpolation was carried out. It is worth remembering that the WWSSN-LP seismometers were acting as a narrow band filter centered at a period of 15 s and with rapid decay toward both the higher and lower frequencies. The gain at 0.01 and 1 Hz is 10 times smaller than that at the central frequency. Therefore, it follows that the analog recordings are a strongly filtered representation of the actual ground motion. For this reason, the digital seismograms have been deconvolved to remove the instrumental response, considering the poles and zeros of the WWSSN-LP seismometers described in the WWSSN data users guide (Peterson and Hutt, 2014). Figure 4 shows the Z (vertical)-component recordings before and after the deconvolution for the instrumental response.

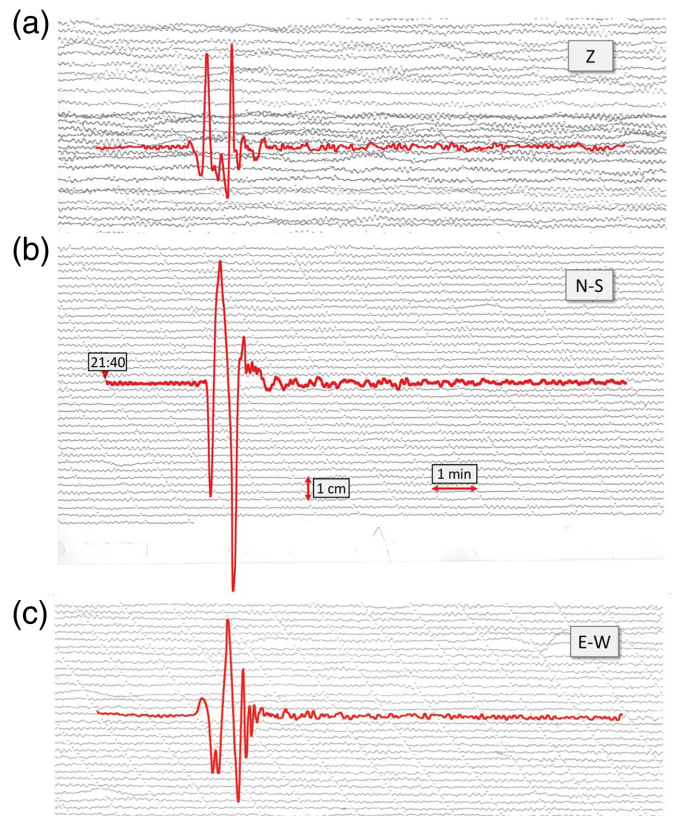
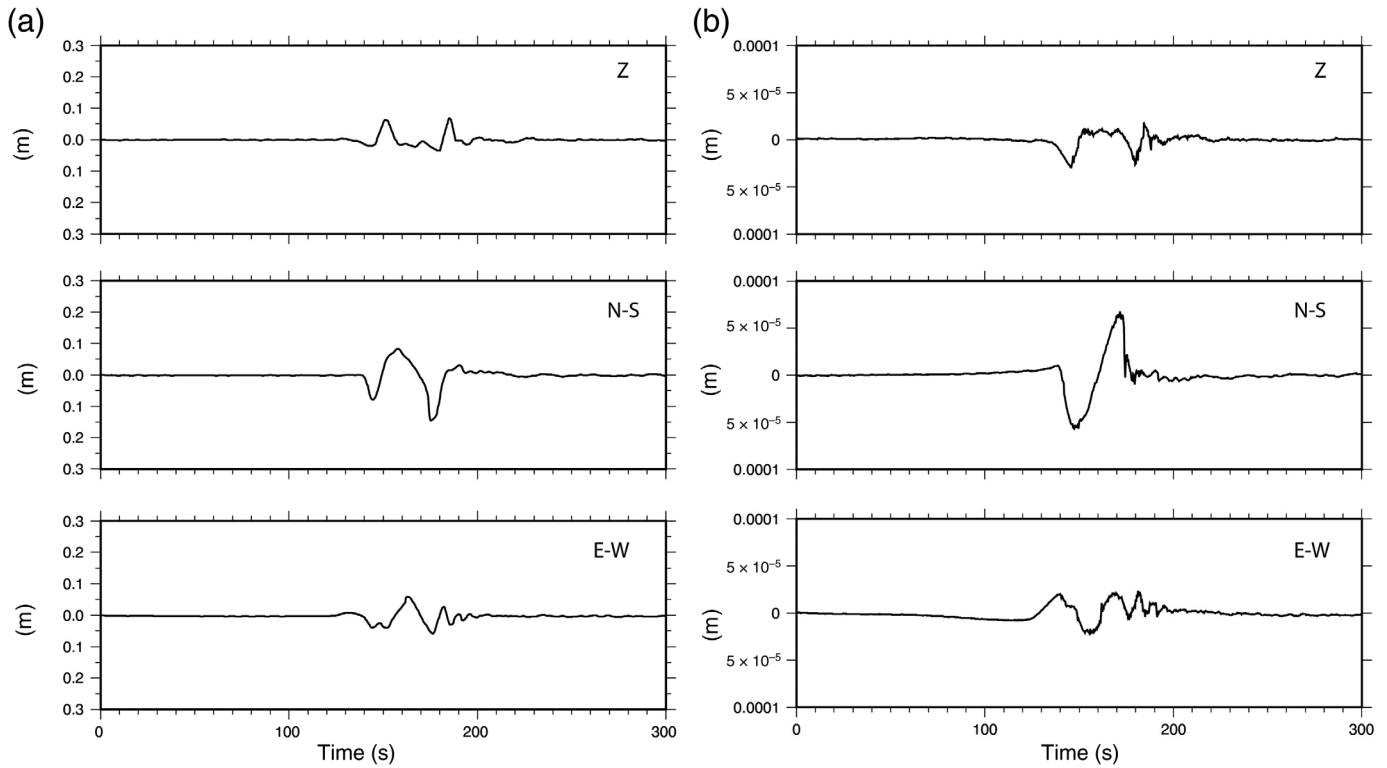


Figure 3. TRI-117 WWSSN long-period recordings of the Vajont event: (a) Z (vertical) component (top), (b) north-south component (middle), and (c) east-west component (bottom). The thick line indicates the part of the seismogram that has been digitized (for each component, this for 12 min). The color version of this figure is available only in the electronic edition.

Clearly, the correction for the instrumental response allows one to enlarge the bandwidth of the signal, affecting not only the polarity of the ground motion but also the amplitude of the different arrivals. It is worth noting that, after the second major event in all components, a dispersive wave train is observable. Finally, the effect of the sensor in filtering the signal seems to have particularly affected the north-south component, in which now a 50 s period (0.02 Hz) becomes dominant. In the case of this component, we suspect that the large amplitude for periods greater than 50 s might be an artifact arising from the instrumental correction. However, in general, the low-frequency signal is consistent with the observation of Lin *et al.* (2015). To better analyze the characteristics of the seismic signal generated by the Vajont event, the digital recordings have been decomposed in the time-frequency domain using the *S* transform (Stockwell *et al.*, 1996). Moreover, to improve the signal-to-noise ratio, the deconvolved seismograms have been suppressed using the approach proposed by Parolai (2009), which is based on a frequency-dependent threshold method that also uses the *S* transform. Figure 5 shows the



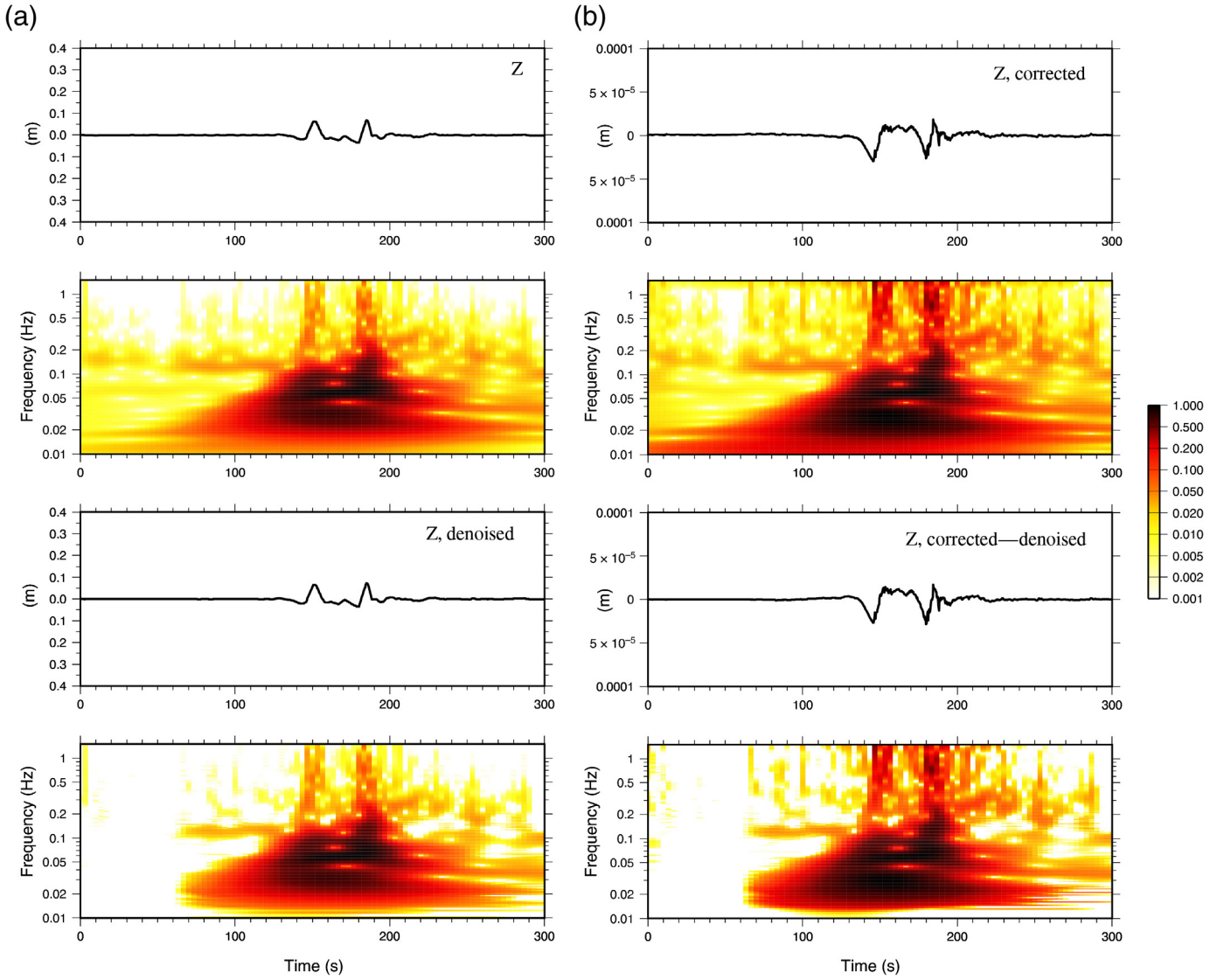
effectiveness of the “denoising” procedure in removing signals not related to the Vajont event. Comparing the results obtained by analyzing the seismograms before (Fig. 5a) and after the deconvolution (Fig. 5b), it is worth noting the extension of the bandwidth after the deconvolution toward both the higher and lower frequencies, the different frequency content of the two main features in the seismograms, and the clearly dispersive behavior of frequencies higher than 0.2 Hz after 200 s. However, although the “denoising” improves the seismic signal, a persistent pre-event disturbance between 0.1 and 0.2 Hz is not fully removed. Figure 6 shows the denoised three-component signals and the corresponding S transform. Although a strong low-frequency signal is affecting all components, spanning the whole duration of the event (although with a slightly smaller duration on the EW component), some differences are noticeable for frequencies higher than 0.1 Hz. In particular, the two perturbations clearly seen on the Z (vertical) recording leave two evident signatures in the time–frequency plot between 140 and 150 s and between 180 and 190 s. This is clearer on the Z and the north–south S transforms. The second event seems to be richer in high-frequency content on the north–south component, while it appears to have a similar importance as the first event on the Z component. This might be related to different mechanisms causing the two events, with the first one related to the landslide movement and the second one due to the mass of water flowing over the dam into the Piave valley. In addition, the arrival of a dispersive wave packet after the second event can be identified. The presence of a similar dispersive signal after the first event

Figure 4. Recordings (a) before and (b) after the correction for the instrumental response. From top to bottom: the Z (vertical), the north–south, and the east–west components, respectively.

cannot be excluded, because it might be masked by the second event’s arrival.

Considerations on the Energy and the Magnitude of the Event

In this analysis, we mainly focus on the first of the two events shown by the seismograms, which is generally considered to be related to the landslide. Taking into account that the volume of the landslide was estimated to be of the order of 270 million m^3 and assuming an average dropping height of 125 m (Weichert *et al.*, 1994; Petronio *et al.*, 2013) and a rock density of 2400 kg/m^3 , it is possible to estimate, in a similar way to what proposed by Ambraseys and Bilham (2012) for the 1911 Sarez, Pamir, landslide, the potential energy of the landslide to be nearly $8 \times 10^{14} \text{ J}$. Considering that it is expected that the landslide might have reached a maximum velocity of 25 m/s leads to the kinetic energy being around $6 \times 10^{14} \text{ J}$. This means that nearly $2 \times 10^{14} \text{ J}$ or 25% is lost to friction. It follows that considering a length of sliding of nearly 400 m and a slope of 37° , the work is consistent with a friction coefficient of 0.29, in excellent agreement with the values presented by Yamada *et al.* (2018). Analyzing the recordings of the station TRI-117, it is possible to estimate the magnitude of an earthquake that would have generated seismic waves of similar amplitude.



We estimated the magnitude considering the formula of [Vanek *et al.* \(1962\)](#), as recommended by the International Association of Seismology and Physics of the Earth's Interior ([Bormann, 2012](#)):

$$M_s = \log(A_H/T)_{\max} + 1.66 \log \Delta + 3.3. \quad (1)$$

Equation (1) has to be used for vectorially combined readings of $(A_H/T)_{\max}$ over the distance range 1° – 160° at periods between $2 \text{ s} < T < 30 \text{ s}$. In this case, the distance between the Vajont site and the seismic station TRI-117 is 1.14° , leading to an M_s equal to 3.7. Similar values (M_d 3.8 and 4.1) have been estimated by calculating the duration magnitude ($\sim 270 \text{ s}$) on the also available (but less clear and not possible to digitize) WWSSN-Short-Period seismograms using the [Suhadolc \(1978\)](#) and [Rebez *et al.* \(1984\)](#) relationships. Using the Gutenberg and Richter relationship ([Gutenberg and Richter, 1956](#)) expressed as

$$\log E_S = 11.8 + 1.5M_s, \quad (2)$$

Figure 5. (a) Z (vertical) component before (top) and after (bottom) the denoising procedure and the corresponding S transform. (b) The Z (vertical) component before (top) and after (bottom) correction for the instrumental response and the corresponding S transform. The color version of this figure is available only in the electronic edition.

in which E_S is given in erg, the energy released as seismic waves from the Vajont event can be estimated to range, considering all the estimated values of M_s , between 2.23×10^{10} and $8.91 \times 10^{10} \text{ J}$, in reasonable agreement with the calculations of [Caloi \(1966\)](#). These values, together with the work that was estimated to have been done by the friction, led to a seismic efficiency of $(1.12 \times 10^{-4} - 4.45 \times 10^{-4})$, which is within the observed range of 10^{-6} – 10^{-3} reported in literature (e.g., [Berrocal *et al.*, 1978](#); [Deparis *et al.*, 2008](#); [Hibert *et al.*, 2011](#); [Levy *et al.*, 2015](#); [Allstadt *et al.*, 2018](#)).

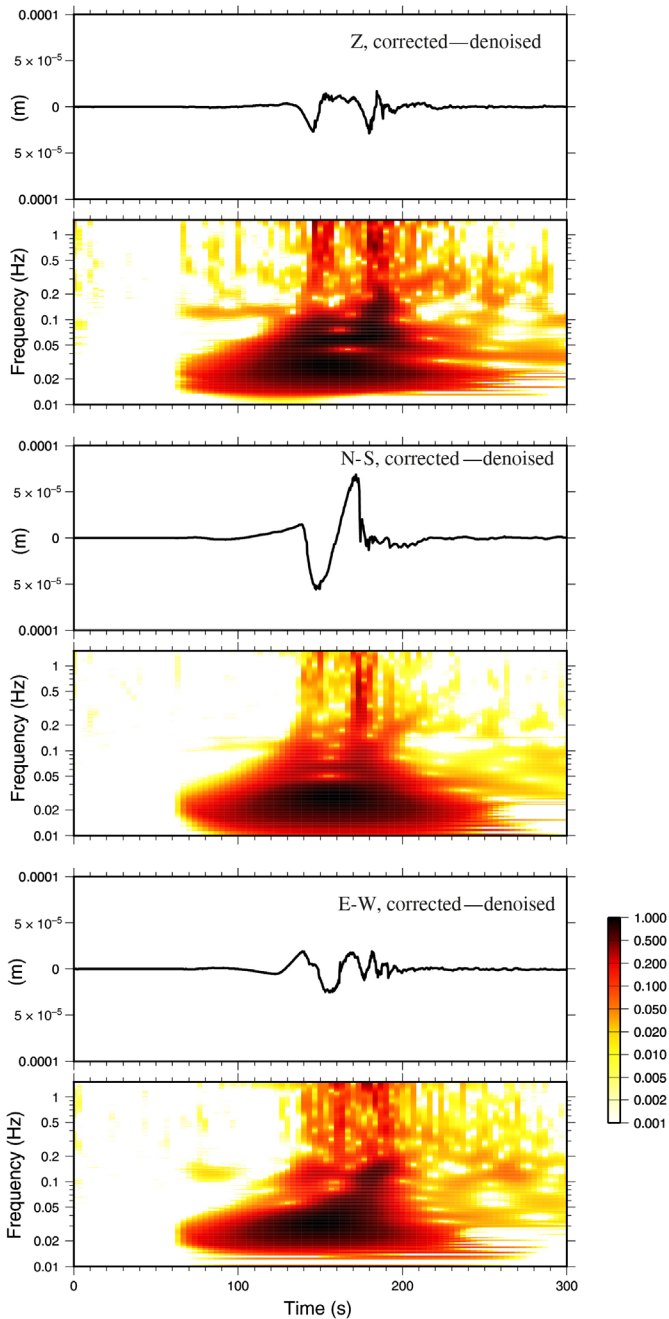


Figure 6. From top to bottom: recordings corrected for the instrumental response and corresponding S transform. From top to bottom: the Z (vertical) component and the corresponding S transform, the north–south component and the corresponding S transform, and the east–west component and the correspondent S transform. The color version of this figure is available only in the electronic edition.

Numerical Simulations

Taking advantage of the excellent knowledge about the Vajont landslide, we now attempt a simulation of the seismic signal induced by the mass movement. The synthetic seismograms are calculated using a semianalytical method that uses an

TABLE 1

Parameters of the Crustal Model Used in the Numerical Simulation

Depth (km)	V_P (km/s)	V_P/V_S	Density (g/cm^3)	Q_P	Q_S
0–2	4.5	1.88	2.45	150	60
2–5	6.5	1.80	2.78	350	140
5–22	6.3	1.79	2.76	300	120
22–35	6.7	1.76	2.91	500	200
35	8.0	1.73	3.10	1000	400

improved Thompson–Haskell propagator matrix algorithm (Wang, 1999). This algorithm avoids numerical instabilities between incident waves from the source at each layer interface by using an orthonormalization approach that is very suitable when the considered models are made up of several layers. Dahlen (1993) showed that a landslide can be represented by a shallow double couple and be modeled as a shallow horizontal thrust fault. Therefore, we considered a thrust fault as a source, oriented with a strike, dip, and rake of 270° , 37° , and 90° , respectively, according to the knowledge about the sliding surface. The source wavelet is described using Brune’s source model (Brune, 1970). However, considering the long duration of the landslide (30 s, Dykes and Bromhead, 2018) compared to that of an earthquake with equivalent magnitude, it would be expected that the creation of waves of similar amplitude, the seismic moment should be increased to reproduce comparable spectral amplitudes. The crustal model of the investigated area, including a softer shallower layer to account for the propagation through the Friuli plain, was adopted from Bressan (2005) and is described in Table 1. Figure 7 shows the recorded seismograms versus the synthetic ones. The horizontal synthetic seismograms have been rotated to be orientated to the north–south and east–west directions for the sake of comparability. The observed seismograms have been high-pass filtered (corner frequency 0.03 Hz) to remove the numerical artifact affecting the north–south component and to facilitate the comparison with the synthetic results, considering frequency bands with similar spectral amplitudes (Fig. 8). Figure 8 shows that the spectral content of the signals is in remarkably good agreement, in particular within the 0.03–0.8 Hz frequency range. The comparison of the calculated and the observed seismograms, which could be carried out only for the first of the two events identified in the real recordings, shows a very good agreement, in particular, for the vertical and the north–south-oriented components. The excellent agreement for the north–south component is obtained only after having inverted the sign of the motion. We carried out several tests to check if any mistake had been made in the numerical

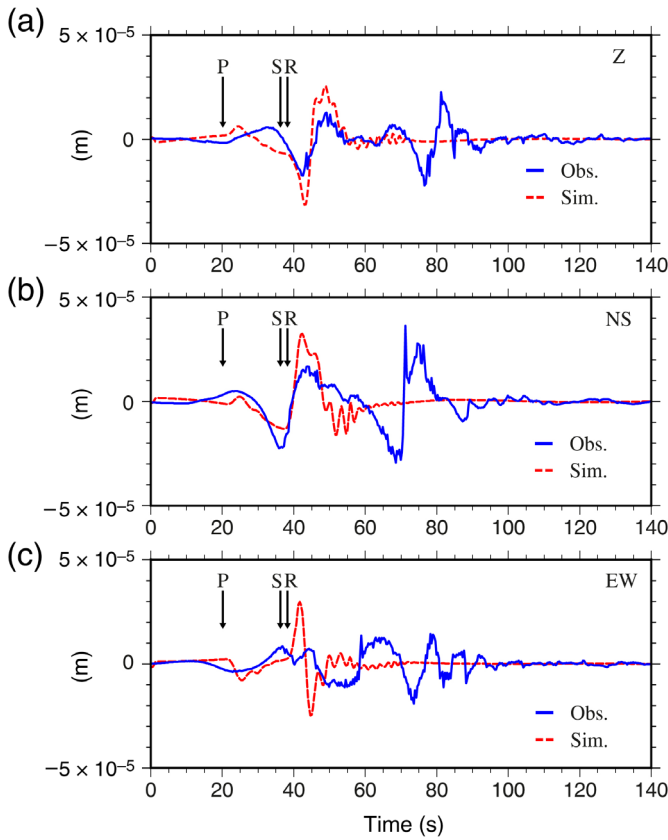


Figure 7. (a) Z (vertical), (b) the north–south, and (c) the east–west synthetic (dashed lines) and observed seismograms. The theoretical arrival times of the P , S , and Rayleigh waves are indicated. Synthetics were only computed for the mass movement event, allowing a direct comparison up to 50–55 s. Obs., observation; Sim., simulation. The color version of this figure is available only in the electronic edition.

simulations, in the real data digitization, or the analysis, but we concluded that perhaps the north–south component of the seismometer was simply inverted. This is not unusual, because other WWSSN-LP recordings have been found to be affected by this problem (J. Schweitzer, personal comm., 2020). It is worth mentioning that to improve the comparability, the synthetic seismograms have been aligned to the observed ones using as references the minimum in the Z components. This allows us to indicate in the figure the expected arrival times for the most important direct phases considering the used model. Furthermore, knowing the absolute Greenwich mean time of the P -wave arrival (estimated considering the difference in time between the minimum and the P -wave arrival on the synthetics) and the theoretical arrival time for the P -wave propagation, given the used crustal model, the origin time of the first (landslide) event was estimated, which was calculated to be 22 hr 41 min 42 s, that is, 12 s after the estimation of Caloi (1966).

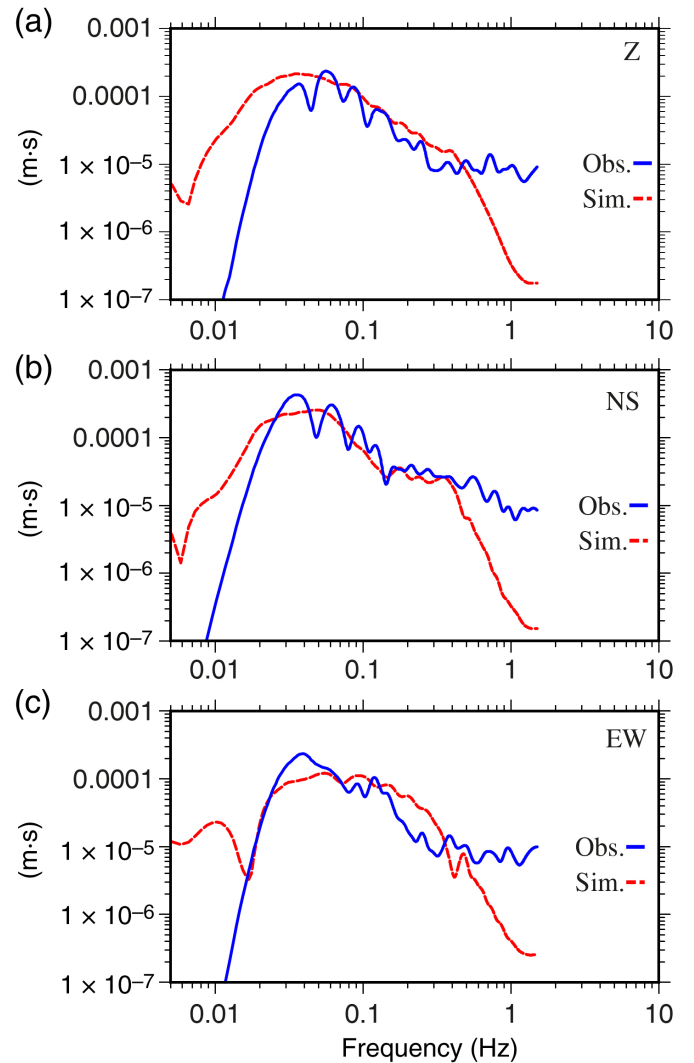


Figure 8. (a) Z (vertical), (b) the north–south, and (c) the east–west component Fourier spectra of the Sim. (dashed lines) and Obs. seismograms. The color version of this figure is available only in the electronic edition.

Conclusions

In this study, we analyzed the recordings of the ground motion induced by the Vajont mountain slide, collected by the TRI-117 station in 1963. The digitalization of the recordings allowed a re-analysis of the event after correcting for the sensor response, which limits the exploitable frequency band and modifies the shape of the time-domain recordings. We estimated that the shaking induced by the landslide event was equivalent to a magnitude ~ 3.7 earthquake based on station TRI-117. However, the magnitude could be better constrained by considering a larger number of recordings. The International Seismological Centre (ISC) bulletin (ISC, 2020) reports an estimation of M_s 5.0 but based on data from only one station (Uppsala, Sweden). A local magnitude M_L 3.5

was estimated by Weichert *et al.* (1994) from macroseismic intensity data. The time–frequency analysis shows also a dispersive wave train (surface waves) generated by the shallow source mechanism associated with both the landslide and the following movement of water. Taking into account the available data on the landslide, the seismic efficiency that we calculated amounts to 1.12×10^{-4} to 4.45×10^{-4} , which falls within the range of the values presented in the literature. We also showed that the ground motion generated by the landslide can be simulated satisfactorily, using a simplified source and crustal model due to the considered frequency range and the corresponding wavelengths of the seismograms. However, our calculations indicated a possible inversion of the recording of one of the components of the WWSSN-LP sensor (which had been installed just before the event). This issue will be investigated in future studies using recordings of strong earthquakes with well-known epicentral locations. Such studies will also be dedicated to advancing the simulations by also considering the second event (the water mass movement) that was recorded by the seismometer. This study confirms that analog seismograms contain valuable information that is not only relevant to earthquakes but also to anthropogenic and other natural events. This information can be better extracted now, taking advantage of digital signal analysis and technological developments not available at the time of the recordings. These encouraging results stimulate two possible developments: (1) the collection of other recordings of the Vajont catastrophe that is available from different European seismological centers to improve the characterization of the event, and (2) the identification of the recordings of the Trieste station of signals related to other large landslides, in particular, those during the 1976 M_L 6.4 Friuli earthquake.

Data and Resources

All data used in this article came from published sources listed in the references. Some plots were made using the Generic Mapping Tools (www.soest.hawaii.edu/gmt, last accessed April 2021; Wessel and Smith, 1998).

Acknowledgments

The authors thank two anonymous reviewers for comments and suggestions that helped in improving the article. The authors thank D. Slejko and G. Renner for the discussions and the information about the Worldwide Standardized Seismographic Station Network (WWSSN) TRI-117 station. The authors thank G. Bressan for the information and discussions regarding the crustal model in the region. N. Casagli provided information and material regarding the Vajont catastrophe. The authors thank J. Parolai for discussions during the estimation of the energy of the event. K. Fleming kindly improved the English language of this article.

References

Allstadt, K. E., R. S. Matoza, A. B. Lockhart, S. C. Moran, J. Caplan-Auerbach, M. M. Haney, W. A. Thelen, and S. D. Malone (2018).

Seismic and acoustic signatures of surficial mass movements at volcanoes, *J. Volcanol. Geoth. Res.* **364**, 76–106, doi: [10.1016/j.jvolgeores.2018.09.007](https://doi.org/10.1016/j.jvolgeores.2018.09.007).

- Alonso, E. E., N. M. Pinyol, and A. M. Puzrin (2010). Catastrophic slide: Vajont landslide, Italy, in *Geomechanics of Failures. Advanced Topics*, Springer, Dordrecht, The Netherlands, doi: [10.1007/978-90-481-3538-7_2](https://doi.org/10.1007/978-90-481-3538-7_2).
- Ambraseys, N., and R. Bilham (2012). The Sarez–Pamir earthquake and landslide of 18 February 1911, *Seismol. Res. Lett.* **83**, no. 2, 294–314, doi: [10.1785/gssrl.83.2.294](https://doi.org/10.1785/gssrl.83.2.294).
- Berrocal, J., A. F. Espinosa, and J. Galdos (1978). Seismological and geological aspects of the Mantaro landslide in Peru, *Nature* **275**, 533–536.
- Bormann, P. (2012). *New Manual of Seismological Observatory Practice (NMSOP-2)*, IASPEI, GFZ German Research Centre for Geosciences, Potsdam, Germany, doi: [10.2312/GFZ.NMSOP-2](https://doi.org/10.2312/GFZ.NMSOP-2).
- Bressan, G. (2005). Modelli monodimensionali di velocità dell'Italia Nord-Orientale OGS, *Internal Report*, 18 pp. (in Italian).
- Brune, J. N. (1970). Tectonic stress and the spectra of seismic shear waves from earthquakes, *J. Geophys. Res.* **75**, 4997–5009.
- Caloi, C. (1966). L'evento del Vajont nei suoi aspetti geodinamici, *Ann. Geophys.* **19**, no. 1, 1–74 (in Italian).
- Dahlen, F. A. (1993). Single-force representation of shallow landslide source, *Bull. Seismol. Soc. Am.* **83**, no. 1, 130–143.
- Deparis, J., D. Jongmans, F. Cotton, L. Baillet, F. Thouvenot, and D. Hantz (2008). Analysis of rock-fall and rock-fall avalanche seismograms in the French Alps, *Bull. Seismol. Soc. Am.* **98**, 1781–1796, doi: [10.1785/0120070082](https://doi.org/10.1785/0120070082).
- Dykes, A. P., and E. N. Bromhead (2018). The Vajont landslide: Re-assessment of the evidence leads to rejection of the consensus, *Landslides* **15**, 1815–1832, doi: [10.1007/s10346-018-0996-y](https://doi.org/10.1007/s10346-018-0996-y).
- Gutenberg, B., and C. F. Richter (1956). Magnitude and energy of earthquakes, *Ann. Geofisc.* **9**, 1–15.
- Hibert, C., A. Mangeney, G. Grandjean, and N. M. Shapiro (2011). Slope instabilities in Dolomieu crater, Réunion Island: From seismic signals to rockfall characteristics, *J. Geophys. Res.* **116**, F04032, 18, doi: [10.1029/2011JF002038](https://doi.org/10.1029/2011JF002038).
- International Seismological Centre (ISC) (2020). On-line bulletin, doi: [10.31905/D808B830](https://doi.org/10.31905/D808B830).
- Levy, C., A. Mangeney, F. Bonilla, C. Hibert, E. S. Calder, and P. J. Smith (2015). Friction weakening in granular flows deduced from seismic records at the Soufrière Hills Volcano, Montserrat, *J. Geophys. Res.* **120**, 7536–7557, doi: [10.1002/2015JB012151](https://doi.org/10.1002/2015JB012151).
- Lin, C. H., J. C. Jan, H. C. Pu, Y. Tu, C. C. Chen, and Y. M. Wu (2015). Landslide seismic magnitude, *Earth Planet. Sci. Lett.* **429**, 122–127, doi: [10.1016/j.epsl.2015.07.068](https://doi.org/10.1016/j.epsl.2015.07.068).
- Parolai, S. (2009). Denoising of seismograms using the S transform, *Bull. Seismol. Soc. Am.* **99**, 226–234, doi: [10.1785/0120080001](https://doi.org/10.1785/0120080001).
- Peterson, J., and C. R. Hutt (2014). World-Wide Standardized Seismograph Network—A data users guide, *U.S. Geol. Surv. Open-File Rept. 2014-1218*, 74 pp., doi: [10.3133/ofr20141218](https://doi.org/10.3133/ofr20141218).
- Petronio, L., J. Boaga, and G. Cassiani (2013). Reflection seismic and surface wave analysis on complex heterogeneous media: The case of mount Toc landslide in the Vajont valley, *Ital. J. Eng. Geol. Environ.* 593–598, doi: [10.4408/IJEGE.2013-06.B-57](https://doi.org/10.4408/IJEGE.2013-06.B-57).
- Pintore, S., M. Quintiliani, and D. Franceschi (2005). Teseo: A vectoriser of historical seismograms, *Comput. Geosci.* **31**, 1277–1285.

- Rebez, A., G. Renner, and D. Slejko (1984). Calcolo della magnitudo locale da durata per la stazione sismologica di Trieste, in *Finalità ed esperienze della Rete Sismometrica del Friuli-Venezia Giulia, Reg. Aut. Friuli-Venezia Giulia*, Trieste, Italy, 29–38 (in Italian).
- Sandron, D., G. F. Gentile, S. Gentili, A. Saraò, A. Rebez, M. Santulin, and D. Slejko (2015). The Wood Anderson of Trieste (NE Italy): One of the last operating torsion seismometers, *Seismol. Res. Lett.* **86**, 1645–1654, doi: [10.1785/0220150047](https://doi.org/10.1785/0220150047).
- Sandron, D., G. Renner, A. Rebez, and D. Slejko (2014). Early instrumental seismicity recorded in the eastern Alps, *Boll. Geof. Teor. Appl.* **55**, no. 4, 755–788.
- Stockwell, R. G., L. Mansinha, and R. P. Lowe (1996). Localization of the complex spectrum: The *S* transform, *IEEE Trans. Signal Process.* **44**, 998–1001.
- Suhadolc, P. (1978). Total durations and local magnitudes for small shocks in Friuli, *Boll. Geof. Teor. Appl.* **20**, 303–312.
- Vanek, J., V. Karnik, A. Zatopek, N. V. Kondorskaya, J. V. Riznichenko, E. F. Savarensky, S. L. Soloviev, and N. V. Shebalin (1962). Standardization of magnitude scale, *Izv. Akad. Nauk. USSR, Ser. Geophys.* **2**, 153–158.
- Wang, R. (1999). A simple orthonormalization method for the stable and efficient computation of Green's functions, *Bull. Seismol. Soc. Am.* **89**, 733–741.
- Weichert, D., R. B. Homer, and S. G. Evans (1994). Seismic signatures of landslides: The 1990 Brenda Mine collapse and the 1965 Hope rockslides, *Bull. Seismol. Soc. Am.* **84**, no. 5, 1523–1532.
- Wessel, P., and W. H. F. Smith (1998). New, improved version of the Generic Mapping Tools released, *Eos Trans. AGU* **79**, 579.
- Yamada, M., A. Mangeney, M. Yuki, and M. Takanori (2018). Estimation of dynamic friction and movement history of large landslides, *Landslides* doi: [10.1007/s10346-018-1002-4](https://doi.org/10.1007/s10346-018-1002-4).